The Silicon Layer Supports Acid Resistance of *Bacillus cereus* Spore

(Running title: a novel acid resistance by Si-encapsulation)

Ryuichi HIROTA[¶], Yumehiro HATA[¶], Takeshi IKEDA, Takenori ISHIDA and Akio KURODA*

Department of Molecular Biotechnology, Graduate School of Advanced Sciences of Matter, Hiroshima University, Higashi-Hiroshima, Hiroshima 739-8530, Japan

October 17, 2009

*To whom correspondence should be addressed.

¶Equal contribution to this work

Tel: +81-82-424-7758, Fax: +81-82-424-7047;

E-mail: akuroda@hiroshima-u.ac.jp

ABSTRACT

Silicon (Si) is considered to be a “quasi-essential” element for most living organisms. However, silicate uptake in bacteria and its physiological functions have remained obscure. We observed that Si is deposited in a spore coat layer covered with nanometer-sized particles in *Bacillus cereus* and that the Si layer enhances acid resistance. The novel acid resistance of the spore mediated by Si-encapsulation was also observed in other *Bacillus* strains, representing a general adaptation enhancing survival under acidic conditions.

INTRODUCTION

Silicon (Si), the second most abundant element in the earth's crust, is an important mineral for living organisms; it acts as a component of the outer skeleton of diatomaceous protozoans (1), as a trace element to help animal bone and teeth development (5) and as an element in plants that enhances their tissue strength and disease resistance (7, 8). These organisms take up silicate from the environment and accumulate it as silica that is formed from highly concentrated silicate (27). In 1980, relatively high concentration of Si was observed at the spore coat region of *Bacillus cereus* and *Bacillus megaterium* spores, by the analysis using scanning transmission electron microscopy (STEM) (14, 23). However, due to the low resolution and relatively weak signal, the precise localization of Si was not determined. On the other hand, the Si contents of *Bacillus coagulans* and *Bacillus subtilis* spores were reported to be almost absent or under the detection limit (4, 24). Some bacteriologists familiar with these data consider the presence of Si an anomaly (17). The presence of Si in bacterial spores (specifically, the spores of *Bacillus anthracis*) became again the focus of attention when anthrax spores were mailed to US Senators in the fall of 2001 (17). The Senate anthrax spores could be easily dispersed as single spores when the container was opened. The investigators considered that coating spores with silica might be involved in preventing

spores from sticking to each other (17). Thus, if silica is normally absent from spores, its presence in *B. anthracis* spores suggested that they had been weaponized (17). Subsequent analysis convinced the investigators that the Si was a natural occurrence (3). However, since silica-rich and -poor spores of the same bacterial strain have never been compared, any relationship between naturally accumulated silica and spore dispersion remained hypothetical.

In the present study, we screened for a bacterium that takes up the highest amount of silicate from among a number of strains isolated from paddy field soil, in order to study Si uptake, to clarify the localization of Si, and to reveal the roles of Si in bacteria. The effect of silica on spore dispersion was also discussed.

MATERIALS AND METHODS

Screening of bacteria that take up silicate. Half of a gram of soil that was collected in a paddy field (Higashi-Hiroshima, Japan) was suspended in 10 ml of sterilized water and mixed well. After serial dilution, the suspensions were spread on an mR2A agar medium (an R2A agar medium (21) supplemented with 0.2 mM $CaCl_2$, 0.01 mM $MnCl_2$, 0.05 mM $ZnCl_2$, 0.05 mM $FeSO_4$) and incubated at 28°C for 48 h. Then, each of the colonies was transferred to a liquid mR2A medium containing 10 μg/ml silicate, and the

silicate concentration after 24- and 48-h incubation was measured by the molybdenum blue assay method (9).

16S rDNA analysis. Universal bacterial 16S rDNA PCR primers 27F (forward primer 5'-AGAGTTTGATCCTGGCTCAG-3') and 1510R (reverse primer 5'-GTCCCGCAACGAGCGCAAC-3') were used to amplify the 16S rDNA (28). DNA sequences were determined with an automated laser fluorescence sequencer (ABI310, Amersham Biosciences) by using the following primers: 27f, 5'-AGAGTTTGATCCTGGCTCAG-3'; rlL, 5'-GTATTACCGCGGCTGG-3'; r2L, 5'-CATCGTTTACGGCGTGGAC-3'; r3L, 5'-TTGCGCTCGTTGCGGGACT-3'; r4L, 5'-ACGGGCGGTGTGTACAAG-3'. The 16S rDNA sequences were aligned by the ClustalW program (25) using default parameters. The program TreeView (20) was used to generate the phylogenetic tree.

Electron microscopy. For scanning electron microscopy with energy dispersive X-ray spectrometry (SEM-EDX) analysis, spores were fixed with 2.5% glutaraldehyde for 6 h at 4°C and dehydrated with ethanol followed by substitution of t-butyl alcohol. After freeze-drying, the spores were analyzed with SEM-EDX (JSM-5900, JEOL, Japan). For

TEM and STEM analysis, spores were prepared by a procedure similar to that used for SEM-EDX, except for the changes of fixation by using cold 2.5% glutaraldehyde, 0.1% $MgSO_4$ in 0.1 M cacodylate buffer (pH 7.2) for 2 h at 4°C and 1% osmium tetraoxide in 0.2 M cacodylate buffer (pH 7.4) for 36 h at 4°C. These spores were suspended in molten 2% agarose. After solidification, part of the agarose containing spores was cut into small cubes, which were dehydrated in ethanol and embedded in epoxy resin. Serial thin sections were prepared and stained with uranyl acetate and lead citrate for structural analysis with TEM (H-9000UHR, Hitachi, Japan). Unstained ultrathin sections were used for STEM-EDX analysis (HD-2000, Hitachi, Japan).

Assays of spore resistance. Bacterial cells were cultured in 100 ml of the mR2A medium for 50 h at 28^{o}C with or without 100 μg/ml silicate. The cultures were centrifuged at 6,000 × *g* for 15 min at 4^{o}C, and each spore pellet was washed twice using equal volume of cold, sterile distilled water. The spores were suspended in a final volume of 10-ml sterile water and kept at 4^{o}C for 1 to 7 days. Microscopic observation indicated that more than 99.8% of cells were refractile spores. The spore solution was diluted to an OD_{600} of 1.0 for the viability tests. The titer in this solution was approximately 10^8 CFU/ml. For wet-heat resistance, spores were incubated in water at

80°C. For UV resistance, spores were irradiated under the UV lamp of a FASIII system (Toyobo, Shiga, Japan) with a maximum output at 254 nm. For hydrogen peroxide resistance, spores were incubated at 28°C in 50 mM K_2HPO_4 buffer (pH 7.5) with 0.5% H_2O_2. For alkaline and acid resistance, spores were centrifuged and resuspended in equal volumes of 0.5 N sodium hydroxide (NaOH), 0.4 N hydrochloric acid (HCl), and 0.1 N nitric acid (HNO_3), respectively. At the indicated times, samples were diluted with cold water and spread on the R2A agar medium. Spore viability was determined by counting the colonies after a 24-h incubation at 28°C.

Hydrogen fluoride treatment. Hydrogen fluoride (HF) was used to dissolve silica of the spore layer. The spore solution diluted to an OD_{600} of 1.0 was centrifuged and the pellet was suspended in equal volumes of 50 mM HF. Silicate released from the spore was measured as described above.

Electrostatic charge. To investigate physical properties of the spores, we prepared spore powder through grinding freeze-dried spores in a mortar. Spore density, which is required for the calculation of electrostatic charge value, was measured by a gas displacement pycnometer (Ultrapycnometer 1000, Quantachrome Instruments, Florida,

USA). Electrostatic charge distribution and diameter of spores was determined using electrical-single particle aerodynamic relaxation time (E-SPART) analyzer (18) (Hosokawa Micron, Osaka, Japan). About 100 mg of the spore powder was shaken in a plastic bag, and then the charges and diameters of individual spores were measured with the E-SPART analyzer. The number of particles counted for each experiment was 3,000.

Nucleotide sequence accession numbers. The 16S rDNA sequence data of YH64 and YH221 have been deposited in the GenBank database under accession no. GQ855295 and GQ855296, respectively.

RESULTS AND DISCUSSION

Screening of bacteria that take up silicate. A total of 240 bacterial colonies were obtained from paddy field soil and transferred to an mR2A medium (an R2A medium supplemented with trace amounts of $CaCl_2$, $MnCl_2$, $ZnCl_2$, and $FeSO_4$) in the presence or absence of 10 μg/ml silicate. Of the 240 isolates, 29 isolates were capable of taking up more than 75% of the silicate from the medium after 48-h incubation (data not shown). The 16S rDNA sequences of these 29 bacteria showed maximum homology to sequences of the genus *Bacillus*, and 21 of these 29 bacteria were homologous to the *B.*

cereus group, a very homogenous cluster of six species: *B. cereus*, *Bacillus thuringiensis*, *B. anthracis*, *Bacillus mycoides*, *Bacillus pseudomycoides*, and *Bacillus weihenstephanensis* (26). The other eight bacteria isolates showed maximum homology to *Bacillus shandongensis* or *Bacillus megaterium*. The bacteria that take up silicate were all phylogenetically classified as the genus *Bacillus*. The strain that takes up the highest amount of silicate among the isolated strains was classified as *B. cereus* based on its 16S rDNA sequence (Fig. 1), being designated as *B. cereus* strain YH64.

To analyze the silicate uptake along with the cell growth, silicate concentration and cellular morphology of the YH64 strain were monitored during incubation on the mR2A medium containing 100 μg/ml silicate (Fig. 2A). After the late logarithmic growth phase (20-40 h), the silicate concentration in the medium decreased drastically. The silicate concentration dropped to ~0.05 μg/ml after 40 h, followed by a slight increase, indicating that a portion of the incorporated silicate was released (Fig. 2A). After 48 h, almost all cells had formed matured spores just after the silicate concentration reached its minimum (Fig. 2B). On the R2A medium that does not contain trace minerals, YH64 did not take up silicate (Fig. 2A) and showed impaired sporulation (approximately 10% of the sporulation efficiency observed in the mR2A medium) (Fig. 2B), indicating that silicate uptake is related to the spore formation.

To determine the relationship between the silicate uptake and spore formation, we measured silicate concentration and the number of heat resistant spores, and confirmed the timing of the appearance of refractile spores during sporulation in the mR2A medium containing 100 μg/ml silicate from 12 to 36 h. Refractile spores appeared at around 16 h (data not shown). Heat resistant spores appeared between 16 h and 18 h (Fig. 2C). Silicate uptake started at around 22 h and more than 90% of silicate was taken up at 36 h. Mother cells still remained at 36 h (data now shown). These results indicated that silicate uptake occurs after the spores acquire heat resistance in their maturing process.

Electron microscopic analysis of the spores. We prepared YH64 spores from the culture using mR2A with or without silicate, and then analyzed them by SEM-EDX. The EDX signal of Si was not observed in the YH64 spores harvested from the culture without silicate; these spores contained almost no or a very low amount of silicate (Fig. 2D), and were denoted as low-Si spores. On the other hand, the Si signal was clearly observed in spores from the culture with silicate (Fig. 2D), and these spores were denoted as high-Si spores. We added silicate to the low-Si spores. The low-Si spores could not take up silicate (data not shown), indicating that silicate was first incorporated

in the mother cell and then accumulated in the spore during maturation.

Previous reports have revealed the presence of Si in the spore coat region of *B. cereus* and *B. megaterium* spores using STEM (14, 23) Since YH64 took up tenfold more silicate than did a *B. cereus* type strain (data shown below), we expected that a relatively strong Si signal should enable us to precisely determine the location of Si. Ultrathin sections of the low- and high-Si YH64 spores were prepared and then analyzed by TEM and STEM-EDX. The spore layer structure (from the outside to the inside of the spore) consists of the exosporium (EX), coat (CT), undercoat (UC), cortex (CX) and core (CR) (2, 6, 11, 12). The EX and UC in the two types of spores appeared the same. However, the CT was thicker in the high-Si spore, and novel nanometer sized-particles (SX) accumulated around the outer side of the CT in the high-Si spore (Fig. 3A and B). SX might correspond to the outer coat layer using the *B. subtilis* analogy (12). Si signal mapping revealed that Si is present in the CT layer and SX particles but not in other regions (Fig. 3C). EDX analysis in CT gave an intense Si signal but no signals for other minerals such as Mn, Zn, Ca and Fe (data not shown).

Comparison of low- and high-Si spores. To investigate the role of Si in spore dispersion, we prepared spore powder through grinding freeze-dried spores in a mortar.

Then we placed 10-mg samples of spore powder into clear 30-ml glass vials and shook them for a few seconds. However, unlike Senate anthrax spores that floated freely (17), both low- and high-Si spores fell quickly to the bottom of the vials and stayed there (data not shown). This result indicated that Si accumulation alone did not make spores dispersible. The electrostatic charge of spores could make them repel one another and thus create self-dispersing spores (17). To test electrostatic charge of spores, we shook the spores in a plastic bag and then applied them to E-SPART analyzer (18). The average electrostatic charges of low- and high-Si spores were almost the same and the individual spore charges showed similar distribution (data not shown). Furthermore, the zeta potentials of the low- and high-Si spores dispersed into water were not significantly different (data not shown). Therefore, the function of Si in bacterial spores had to be reconsidered.

The Si layer supports acid resistance of the spores. Spores can survive under conditions unsuitable for growth and resist various kinds of stress. The spore coat is related to the impermeability to the spore's inner membrane; thus, the spore coat is thought to confer resistance to toxic chemicals (19). We compared the sensitivity of YH64 low- and high-Si spores to wet-heat, UV irradiation, 5.0% H_2O_2, 0.5 N NaOH,

and 0.4 N HCl. Only the viability of the high-Si spores under the acidic condition was increased as compared to that of the low-Si spores (Fig. 4A to E). The viability of high-Si spores treated with a different acid solution (0.1 N HNO_3) was also higher than that of low-Si spores (Fig. 4F), indicating that the Si layer confers general acid resistance.

Next, we examined the acid resistance of another isolated strain, YH221, whose 16S rDNA sequence shared 99% identity with that of *B. shandongensis* (Fig. 1). YH221 took up one-seventh of the silicate compared to YH64 (Fig. 5). Surprisingly, high-Si YH221 spores had 1,000 times the survival rate of the low-Si spores after a 3-h incubation in 0.2 N HCl (Fig. 6A). Then, we prepared YH221 spores under various silicate concentrations and examined their acid resistance. The acid resistance increased with increasing amounts of Si uptake (Fig. 6B). We examined silicate uptake in *Bacillus*-type strains deposited in the NITE Biological Resource Center (NBRC, Japan). *B. cereus* NBRC15305, *B. thuringiensis* NBRC101235 and *B. megaterium* NBRC15308 took up approximately 0.03, 0.10, and 0.05 pg silicate per spore, respectively (Fig. 5). However, almost no silicate uptake was observed in *B. subtilis* 168 and *B. mycoides* NBRC 101228 under this condition (Fig. 5). The YH64 strain took up 15 times as much silicate (0.49 pg Si/spore, corresponding to approximately 6.3% dry weight) as its

closest relative, *B. cereus* NBRC15305, in spite of more than 99% 16S rDNA identity between these two strains. Indeed, the morphological characteristics of the cells as observed under microscopy and the characteristics of colony form of *B. cereus* YH64 and NBRC 15305 were different. We examined HCl resistance of *B. cereus* NBRC15305 and *B. thuringiensis* NBRC101235 spores. As expected, the high-Si spores were more resistant to HCl than the low-Si spores (data not shown). Not all *Bacillus* strains take up silicate. However, it seems highly likely that the acid resistance conferred by Si-encapsulation is a general phenomenon of *Bacillus* strains that take up silicate.

Strong mineral acids rupture *Bacillus* spores by breaking down spore permeability barriers (22). Most acidophilic organisms have evolved extremely efficient mechanisms to pump protons out of the intracellular space to maintain the cytoplasm at near neutral pH (15). However, the spore is metabolically inactive before germination. The Si-encapsulation, probably as silica (discussed below) that is resistant to most acids, may decrease the proton permeability of the spore coat and confer acid resistance to the spores. Interestingly, the Si-encapsulation of an inorganic pigment, Ultramarine Blue, enhances acid resistance and overcomes the limitations on the use of the pigment (10).

As far as we know, diatoms, plants, and animals accumulate silicate as silica (13).

Silica can be dissolved in hydrogen fluoride (HF) (16). Accordingly, if the Si layer of spore contains silica, it could be removed from the high-Si spores with HF treatment. Approximately 75% of Si that was accumulated in the spores was released as silicate after 50 mM HF treatment (data not shown). We compared the acid resistance of HF-treated high Si- and low-Si spores (Fig. 7). After HF treatment, the viability of the high-Si spores was no longer higher than that of the low-Si spores. These results indicated that the Si layer mainly contains silica and supports acid resistance.

Si is naturally available in soil and water. The silicate concentration in soil ranges from 0.1 to 0.6 mM (9.6 to 57.7 μg/ml) (7). Therefore, the acid resistance conferred by Si-encapsulation may occur in nature. Spores may encounter strong acids in environments such as the digestive conditions in animal stomachs (around 0.1 N HCl), indicating that a physiological function of Si in bacteria may be to aid survival under these conditions. When the anthrax powder sent to the US Senate in 2001 was found to be coated with unusual silica, it was discussed whether the silica was related to spore dispersion. We concluded that Si-encapsulation is not sufficient to make spores dispersible but does contribute to survival under acidic conditions. Our findings also strongly indicate that the anthrax spores were harvested from culture on a silicate-containing medium.

ACKNOWLEDGEMENT

This work was supported in part by the Solution Oriented Research for Science and Technology Program (PREST-SORST) of the Japan Science and Technology Agency.

REFERENCES

1. **Azam, F., B. B. Hemmingsen, and B. E. Volcani.** 1974. Role of silicon in diatom metabolism. V. Silicic acid transport and metabolism in the heterotrophic diatom *Nitzschia alba*. Arch. Microbiol. **97:**103-14.

2. **Ball, D. A., R. Taylor, S. J. Todd, C. Redmond, E. Couture-Tosi, P. Sylvestre, A. Moir, and P. A. Bullough.** 2008. Structure of the exosporium and sublayers of spores of the *Bacillus cereus* family revealed by electron crystallography. Mol. Microbiol. **68:**947-58.

3. **Bhattacharjee, Y., and M. Enserink.** 2008. "Anthrax Investigation". Science **321:**1026-1027.

4. **Carroll, A. M., M. Plomp, A. J. Malkin, and P. Setlow.** 2008. Protozoal digestion of coat-defective *Bacillus subtilis* spores produces "rinds" composed of insoluble coat protein. Appl. Environ. Microbiol. **74:**5875-81.

5. **Chumlea, W. C.** 2007. Silica, a mineral of unknown but emerging health importance. J. Nutr. Health Aging **11:**93.

6. **Driks, A.** 1999. *Bacillus subtilis* spore coat. Microbiol. Mol. Biol. Rev. **63:**1-20.

7. **Epstein, E.** 1994. The anomaly of silicon in plant biology. Proc. Natl. Acad. Sci. USA **91:**11-7.

8. **Fauteux, F., W. Remus-Borel, J. G. Menzies, and R. R. Belanger.** 2005. Silicon and plant disease resistance against pathogenic fungi. FEMS Microbiol. Lett. **249:**1-6.

9. **Franklin, A. D., and S. S. Yamamura.** 1970. Versatile spectrophotpmetric method for the determination of silicon. Talanta **17:**143-149.

10. **Guiqin, Y., L. Xiaozeng, Y. Lemei, C. Jianzhong, and G. Congrong.** 1996. Microencapsulation of ultramarine particles in water/oil emulsion and surface fractal dimentionality of the particles. Dyes and Pigments **34:**57-62.

11. **Henriques, A. O., and C. P. Moran, Jr.** 2000. Structure and assembly of the bacterial endospore coat. Methods **20:**95-110.

12. **Henriques, A. O., and C. P. Moran, Jr.** 2007. Structure, assembly, and function of the spore surface layers. Annu. Rev. Microbiol. **61:**555-88.

13. **Iler, R. K.** 1979. Silica in biology, The chemistry of silica: solubility, polymerization, colloid and surface properties and biochemistry of silica. Wiley-Interscience, Malden, MA.

14. **Jonhstone, K., D. J. Ellar, and T. C. Appleton.** 1980. Location of metal ions in *Bacillus megaterium* spores by high-resolution electron probe X-ray microanalysis. FEMS Microbiol. Lett. **7:**97-101.

15. **Konings, W. N., S. V. Albers, S. Koning, and A. J. Driessen.** 2002. The cell membrane plays a crucial role in survival of bacteria and archaea in extreme environments. Antonie Van Leeuwenhoek **81:**61-72.

16. **Kröger, N., R. Deutzmann, and M. Sumper.** 1999. Polycationic peptides from diatom biosilica that direct silica nanosphere formation. Science **286:**1129-32.

17. **Matsumoto, G.** 2003. Bioterrorism. Anthrax powder: state of the art? Science **302:**1492-7.

18. **Matsusaka, S., M. Oki, and H. Masuda.** 2003. Bipolar charge distribution of a mixture of particles with different electrostatic characteristics in gas-solids pipe flow. Powder Technology **135:**150-155.

19. **Nicholson, W. L., N. Munakata, G. Horneck, H. J. Melosh, and P. Setlow.** 2000. Resistance of *Bacillus* endospores to extreme terrestrial and extraterrestrial environments. Microbiol. Mol. Biol. Rev. **64:**548-72.

20. **Page, R. D.** 1996. TreeView: an application to display phylogenetic trees on personal computers. Comput. Appl. Biosci. **12:**357-8.

21. **Reasoner, D. J., and E. E. Geldreich.** 1985. A new medium for the enumeration and subculture of bacteria from potable water. Appl. Environ. Microbiol. **49:**1-7.

22. **Setlow, B., C. A. Loshon, P. C. Genest, A. E. Cowan, C. Setlow, and P. Setlow.** 2002. Mechanisms of killing spores of *Bacillus subtilis* by acid, alkali and ethanol. J. Appl. Microbiol. **92:**362-75.

23. **Stewart, M., A. P. Somlyo, A. V. Somlyo, H. Shuman, J. A. Lindsay, and W. G. Murrell.** 1980. Distribution of calcium and other elements in cryosectioned *Bacillus cereus* T spores, determined by high-resolution scanning electron probe x-ray microanalysis. J. Bacteriol. **143:**481-91.

24. **Stewart, M., A. P. Somlyo, A. V. Somlyo, H. Shuman, J. A. Lindsay, and W. G. Murrell.** 1981. Scanning electron probe x-ray microanalysis of elemental distributions in freeze-dried cryosections of *Bacillus coagulans* spores. J. Bacteriol. **147:**670-4.

25. **Thompson, J. D., D. G. Higgins, and T. J. Gibson.** 1994. CLUSTAL W: improving the sensitivity of progressive multiple sequence alignment through sequence weighting, position-specific gap penalties and weight matrix choice. Nucleic Acids Res. **22:**4673-80.

26. **Vilas-Boas, G. T., A. P. Peruca, and O. M. Arantes.** 2007. Biology and taxonomy of *Bacillus cereus, Bacillus anthracis,* and *Bacillus thuringiensis*. Can. J. Microbiol. **53:**673-87.

27. **Volcani, B. E.** 1981. Cell wall formation in diatoms. *In* T. L. Simpson and B. E. Volcani (ed.), Silicon and siliceous structures in biological systems. Springer New York Inc.

28. **Weisburg, W. G., S. M. Barns, D. A. Pelletier, and D. J. Lane.** 1991. 16S ribosomal DNA amplification for phylogenetic study. J. Bacteriol. **173:**697-703.

FIGURE LEGENDS

Fig. 1. A phylogenetic tree of isolated bacteria (YH64, YH221) and their related strains based on 16S rDNA sequence. Distances were calculated from nucleic acid sequences by using the ClustalW program. The 16S rDNA sequences were obtained from the NCBI GenBank database (*B. cereus* [AB247137.1], *B. thuringiensis* [EF537013.1], *B. anthracis* [AY138382.1], *B. subtilis* [AY833569.1], *B. samanii* [EF036537.1], *B. mycoides* [AF65957.1], *B. pseudomycoides* [AM747227.1], *B. megaterium* [AB271751.1], *B. haldurans* [EF113314.1], *B. shandongensis* [EU046267.1], *B. luciferensis* [DQ870692.1], *B. clausii* [AY960115.1], *B. licheniformis* [AY017347], *B. simplex* [D78478], *B. fastidiosus* [X60615], *B. coagulans* [AB116143.1]). The scale bar indicates substitutions per site.

Fig. 2. Silicate uptake during *B. cereus* YH64 growth. (A) Growth of YH64 (closed circles) on mR2A (left) and R2A (right) media containing 100 μg/ml silicate and silicate concentrations in the medium (open squares) were measured at different time points. **(B)** Phase contrast microscopic images of YH64 that grew on mR2A and R2A media. Scale bar, 10 μm. **(C)** Silicate concentration (open squares) and the number of heat resistant spores (closed triangles) of YH64 culture containing 100 μg/ml silicate. The cell suspension was heated at 65^{o}C for 30 min and the number of heat resistant spores that formed colonies on R2A agar plate was determined. **(D)** EDX spectrum of YH64 spores. The EDX signal of silicon is indicated by an arrowhead. Insets are the scanning electron microscopic images of the spores. Scale bars, 1 μm.

Fig. 3. Layer structure and Si localization of the YH64 spore. (A) TEM images of ultrathin section of low- and high-Si spores stained with uranium and lead. EX, exosporium; CT, coat; UC, undercoat; CX, cortex; CR, core; Nanometer-sized particles (SX) were observed around the outer side of the CT layer of the high-Si spore. The rectangular region was enlarged, and a schematic illustration of the layer structure is shown below the individual images. A red line indicates the edge of the CT layer. Scale

bars, 100 nm. **(B)** Thickness of the CT layer of low- and high-Si spores was measured by using three spore images. The data represent the mean and standard deviation. **(C)** Si localization of the high-Si spore. Unstained ultrathin sections of the high-Si spore were used for STEM-EDX analysis to identify the location of Si in the spores. TEM image, Si map (green), and a merged picture are shown. Scale bar, 100 nm.

Fig. 4. Viability of YH64 spores under various stress conditions. Resistance of low- and high-Si spores to wet-heat **(A)**, UV **(B)**, hydrogen peroxide **(C)**, alkaline **(D)** and acid **(E, F)** were assayed as described in MATERIALS AND METHODS. Symbols: closed circle, high-Si spores; open circle, low-Si spores. Data represent the mean and standard deviation of at least three independent experiments.

Fig. 5. Si content of various *Bacillus* spores. The amounts of silicate per spore were measured in *B. subtilis* 168, *B. cereus* NBRC15308, *B. thuringiensis* NBRC101235, *B. mycoides* NBRC101228, *B. megaterium* NBRC15308, and bacteria isolated in this study (YH64, YH221).

Fig. 6. HCl resistance of YH221 spores. (A) Low- and high-Si spores were prepared

from 50-h cultures, washed two times with sterilized water, and suspended in 0.2 N HCl. The viability was determined as described above. Symbols: closed circle, high-Si spores; open circle, low-Si spores. Data represent the mean and standard deviation of at least three independent experiments. **(B)** The effect of Si content in YH221 spore on the survival rate after HCl treatment. YH221 spores containing different amounts of silicate were prepared. The viability of the spores after a 2-h incubation in 0.2 N HCl was determined.

Fig. 7. HCl resistance of low- and high-Si spores after HF treatment. Low- and high-Si YH64 spores treated with 50 mM HF for 10 min were suspended in 0.4 N HCl. Symbols: closed circle, high-Si spores; open circle, low-Si spores. Data represent the mean and standard deviation of three independent experiments.

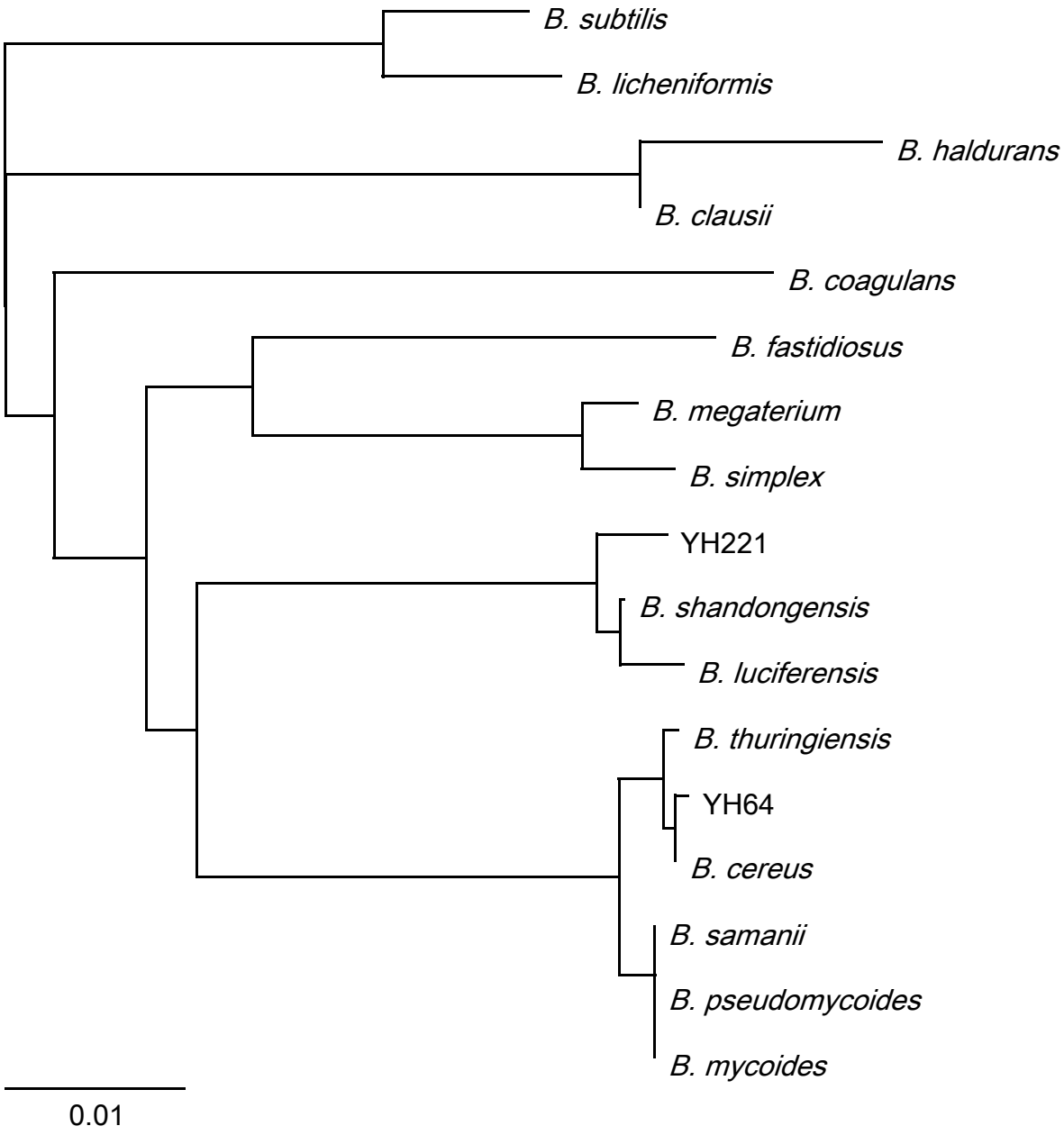

Figure 1. Hirota et al.

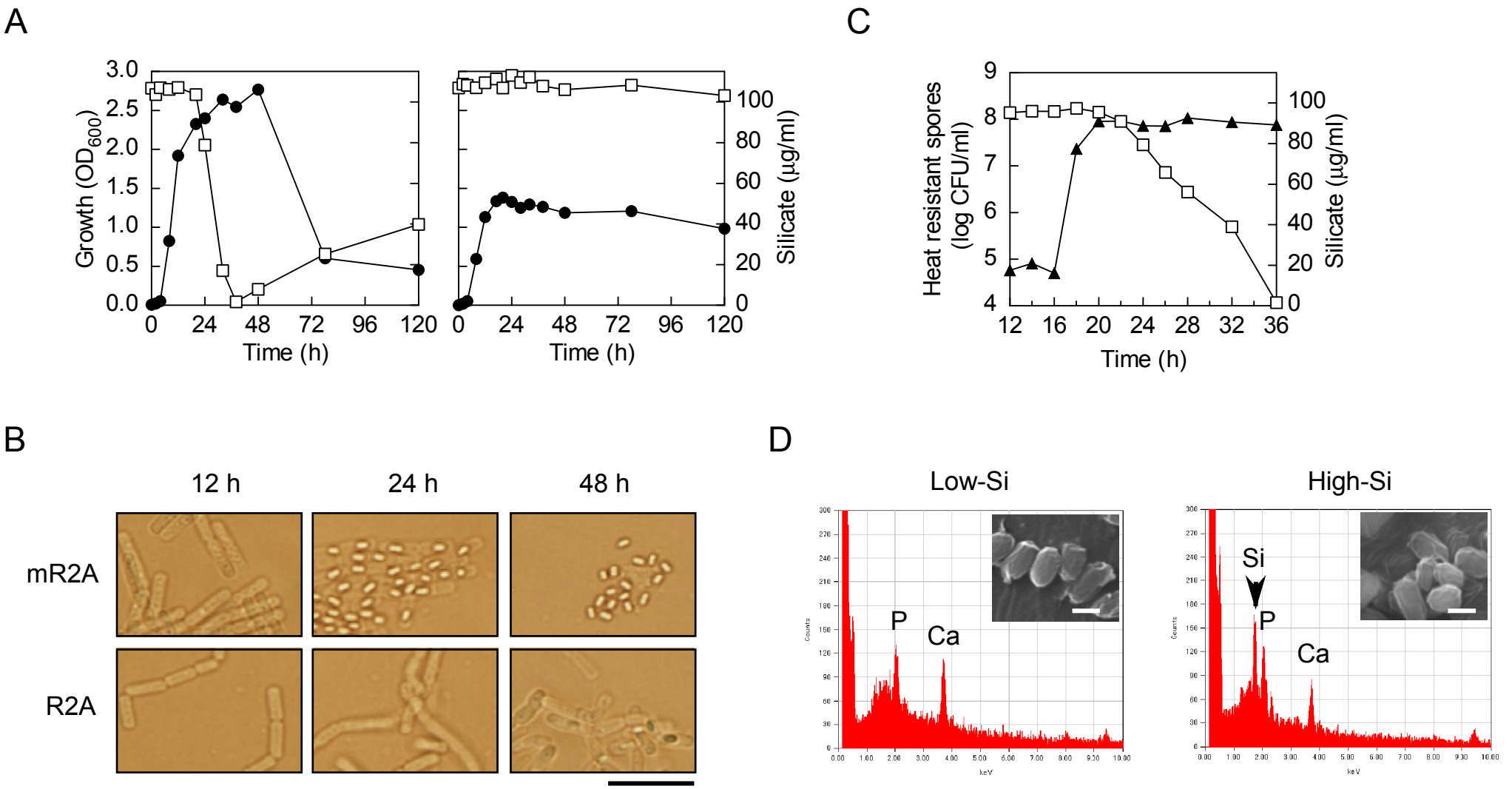

Figure 2. Hirota et al.

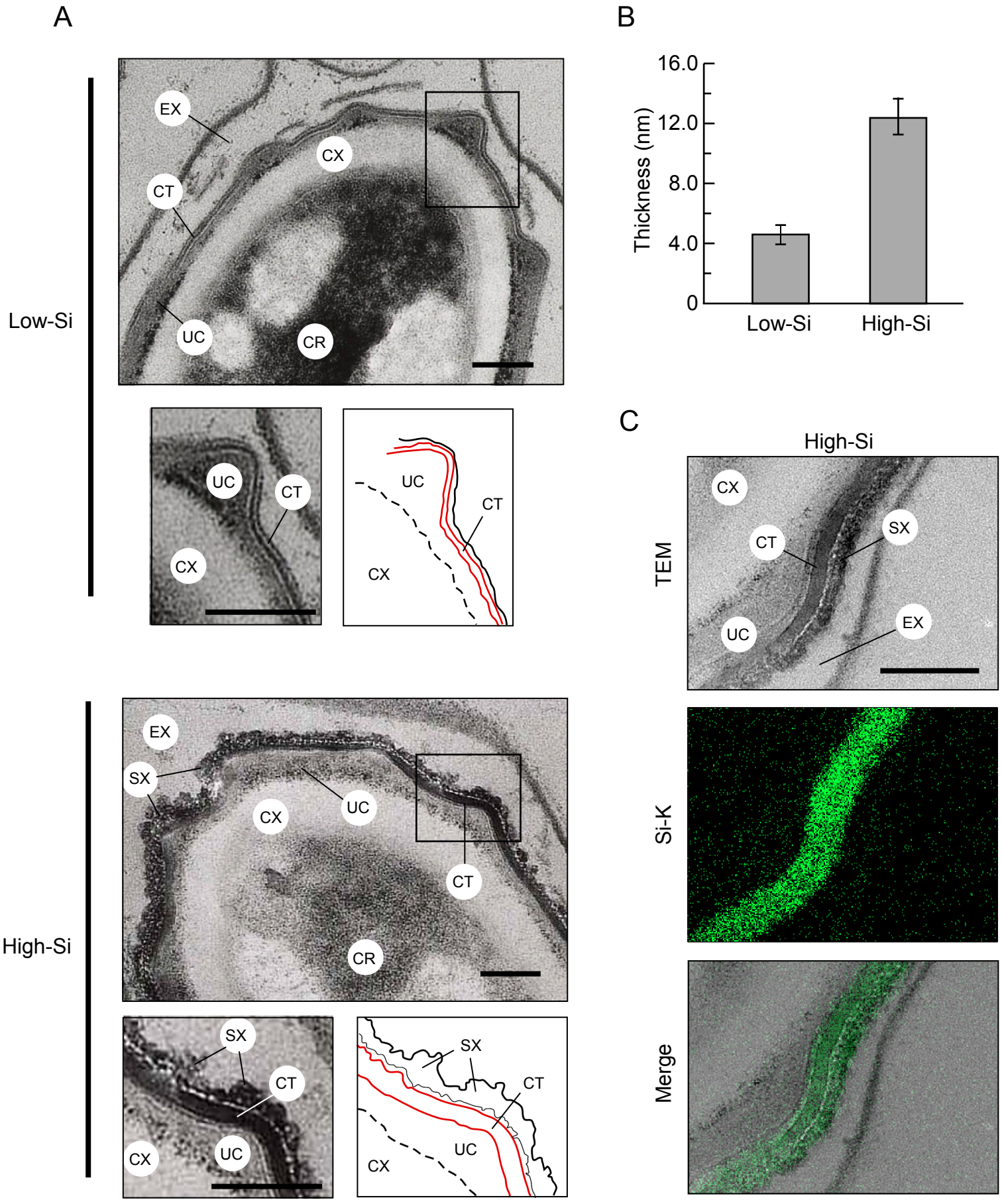

Figure 3. Hirota et al.

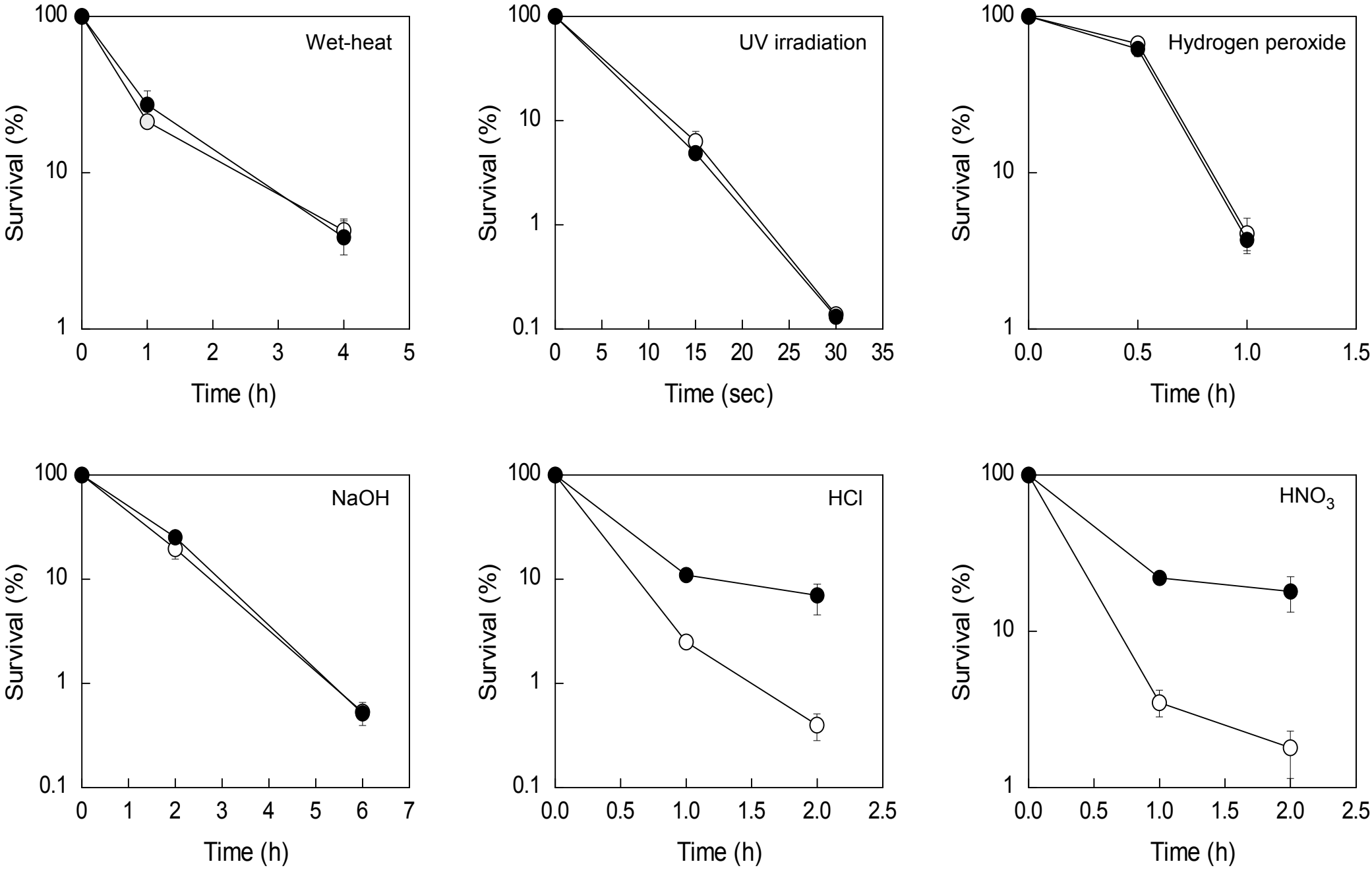

Figure 4. Hirota et al.

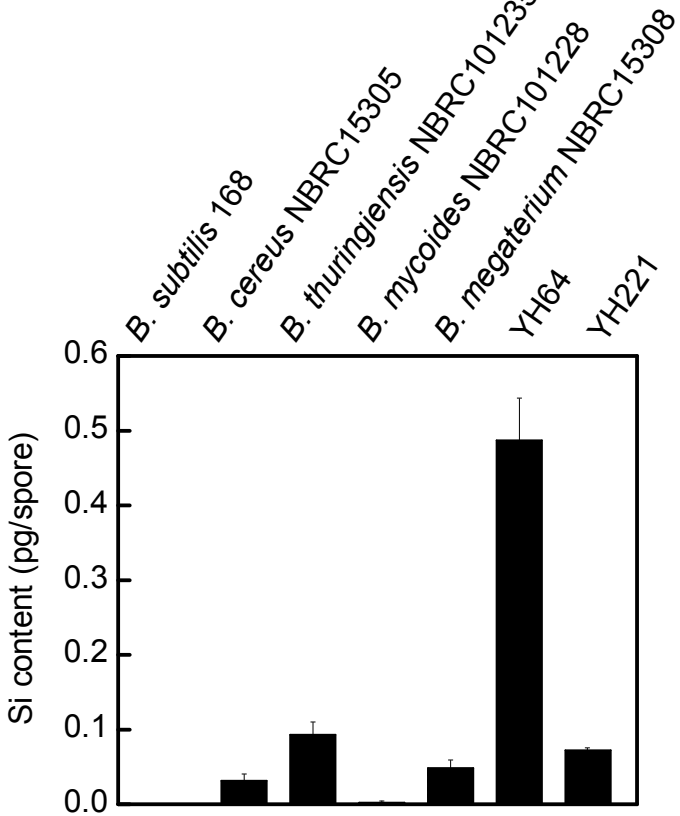

Figure 5. Hirota et al.

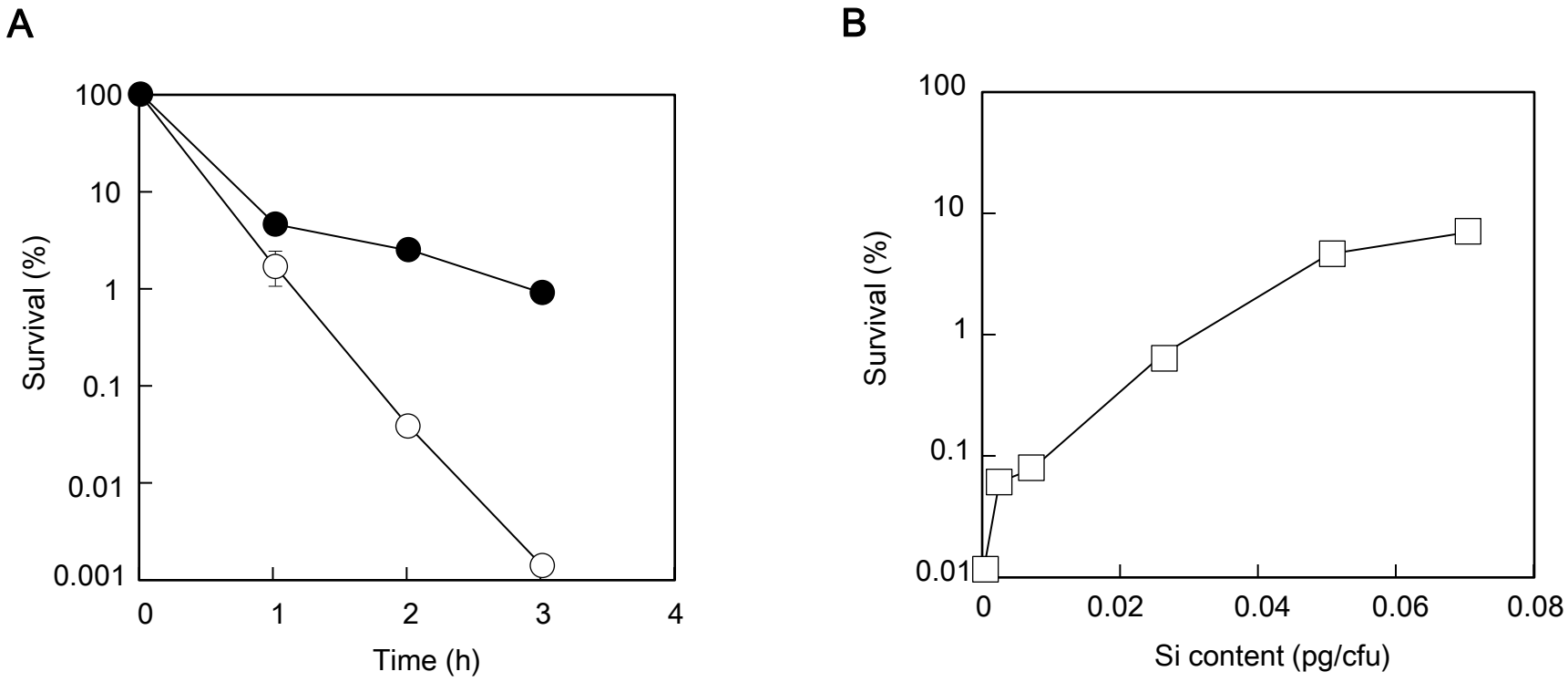

Figure 6. Hirota et al.

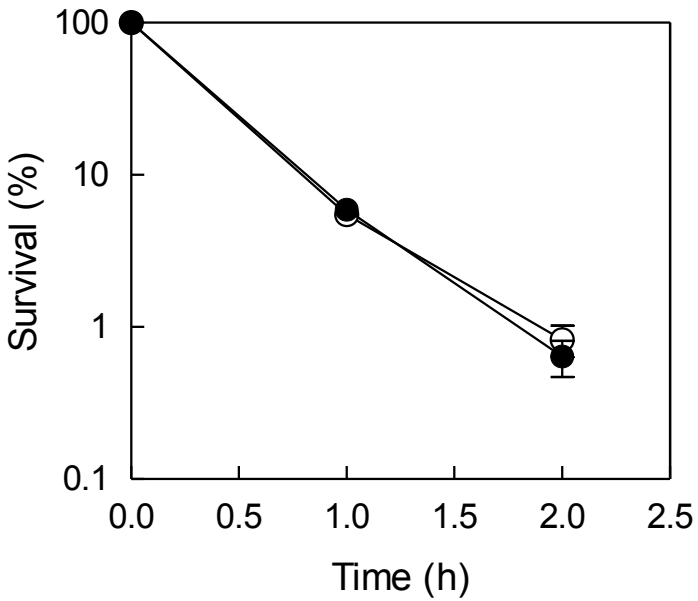

Figure 7. Hirota et al.